The EMBO Journal Vol. 21 No. 14 pp. 3728–3738, 2002

Essential role of PDK1 in regulating cell size and development in mice

Margaret A.Lawlor[1], Alfonso Mora, Peter R.Ashby[2], Michayla R.Williams, Victoria Murray-Tait[3], Lorraine Malone[3], Alan R.Prescott[3], John M.Lucocq[3] and Dario R.Alessi

MRC Protein Phosphorylation Unit, [2]Cell and Developmental Biology and [3]Division of Cell Biology and Immunology, School of Life Sciences, MSI/WTB Complex, University of Dundee, Dow Street, Dundee DD1 5EH, UK

[1]Corresponding author
e-mail: m.a.lawlor@dundee.ac.uk

PDK1 functions as a master kinase, phosphorylating and activating PKB/Akt, S6K and RSK. To learn more about the roles of PDK1, we generated mice that either lack PDK1 or possess PDK1 hypomorphic alleles, expressing only ~10% of the normal level of PDK1. PDK1$^{-/-}$ embryos die at embryonic day 9.5, displaying multiple abnormalities including lack of somites, forebrain and neural crest derived tissues; however, development of hind- and midbrain proceed relatively normally. In contrast, hypomorphic PDK1 mice are viable and fertile, and insulin injection induces the normal activation of PKB, S6K and RSK. Nevertheless, these mice are 40–50% smaller than control animals. The organ volumes from the PDK1 hypomorphic mice are reduced proportionately. We also establish that the volume of a number of PDK1-deficient cells is reduced by 35–60%, and show that PDK1 deficiency does not affect cell number, nuclear size or proliferation. We provide genetic evidence that PDK1 is essential for mouse embryonic development, and regulates cell size independently of cell number or proliferation, as well as insulin's ability to activate PKB, S6K and RSK.

Keywords: cell growth/cell size/embryonic development/PDK1/PKB–Akt/PI 3-kinase

Introduction

The 3-phosphoinositide-dependent protein kinase-1 (PDK1) plays a key role in regulating the activity of a group of insulin and growth factor-stimulated protein kinases that belong to the AGC subfamily of protein kinases (Niederberger and Schweingruber, 1999; Toker and Newton, 2000; Alessi, 2001). These include isoforms of protein kinase B (PKB, also known as Akt) (Brazil and Hemmings, 2001; Scheid and Woodgett, 2001), p70 ribosomal S6 kinase (S6K) (Avruch *et al*., 2001; Volarevic and Thomas, 2001) and p90 ribosomal S6 kinase (Frodin *et al*., 2000). Once activated, these enzymes mediate many of the diverse effects of insulin and growth factors on cells by phosphorylating key regulatory proteins that play important roles controlling processes such as cell survival, proliferation, nutrient uptake and storage.

There is only a single gene encoding PDK1 in mammals. PDK1 functions to activate AGC kinase members by phosphorylating these enzymes at a conserved residue known as the T-loop residue, which is located in the core of their kinase catalytic domain (Niederberger and Schweingruber, 1999; Toker and Newton, 2000; Alessi, 2001). The activation of PKB and S6K by PDK1 is dependent on prior activation of the phosphoinositide 3-kinase (PI 3-kinase). This produces the second messenger, phosphatidylinositol 3,4,5-trisphosphate [PtdIns(3,4,5)P_3], which binds to the pleckstrin homology domains of PKB and PDK1, recruiting these enzymes to the plasma membrane where PKB is phosphorylated by PDK1 (Brazil and Hemmings, 2001; Scheid and Woodgett, 2001). In contrast, S6K does not interact with PtdIns(3,4,5)P_3 but, instead, PtdIns(3,4,5)P_3 stimulates the phosphorylation of a Thr residue located C-terminal to the S6K catalytic domain in a motif known as the hydrophobic motif, by an as yet unknown mechanism (Avruch *et al*., 2001; Volarevic and Thomas, 2001). The phosphorylation of S6K at this site enhances the ability of PDK1 to interact with, phosphorylate and activate S6K (Biondi *et al*., 2001). The activation of RSK isoforms is initiated by ERK/MAP kinase phosphorylation in response to agonists that activate the Ras/Raf pathway. In order for RSK to be activated by ERK, RSK also needs to be phosphorylated at the T-loop residue of its N-terminal kinase domain by PDK1 (Frodin and Gammeltoft, 1999).

The key role that PDK1 plays in activating certain AGC kinase members was established by the finding that mouse embryonic stem (ES) cells lacking PDK1 failed to activate PKB, S6K and RSK in response to stimuli that trigger the activation of these enzymes in wild-type ES cells (Williams *et al*., 2000). It was perhaps unexpected that ES cells lacking PDK1 were viable, because PKB and RSK have been reported to play important roles in regulating survival and proliferation in other cell types (Nebreda and Gavin, 1999; Lawlor and Alessi, 2001). Furthermore, knocking out PDK1 homologues in *Saccharomyces cerevisiae* (Casamayor *et al*., 1999; Inagaki *et al*., 1999), *Schizosaccharomyces pombe* (Niederberger and Schweingruber, 1999), *Caenorhabditis elegans* (Paradis *et al*., 1999) and *Drosophila* (Cho,K.S. *et al*., 2001; Rintelen *et al*., 2001) have revealed that PDK1 is required for the normal development and viability of these organisms. To learn more about the roles that PDK1 plays in mammals, we generated and analysed the phenotype of both PDK1 knockout mice and PDK1 hypomorphic mutant mice that express markedly lower levels of PDK1 in all tissues examined.

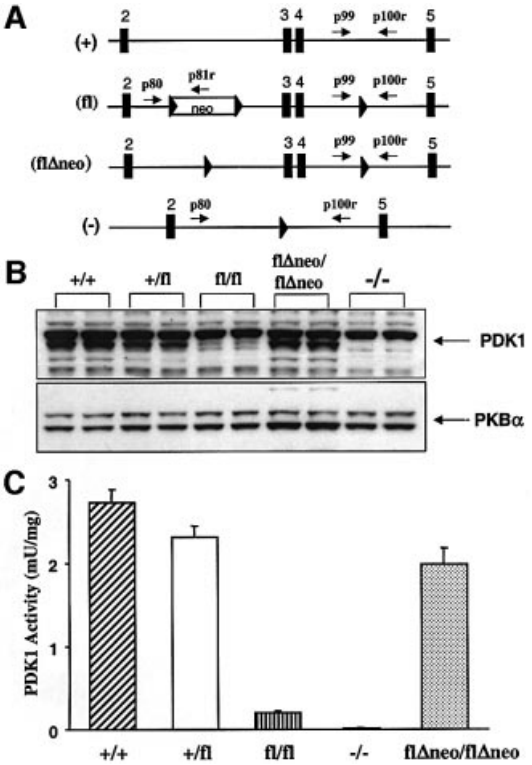

Fig. 1. Generation of hypomorphic PDK1 ES cells. (**A**) Diagram illustrating the 5′ end of the *PDK1* gene and the different alleles that we have generated. The black boxes represent exons, continuous lines represent introns, triangles represent *loxP* sites and the neo box represents a neomycin resistance gene cassette. The positions of the PCR primers used to genotype the ES cells and mice are indicated with arrows. +, wild-type allelle; fl, allelle containing the neomycin resistance gene flanked with *loxP* sites between exons 2 and 3 as well as a *loxP* site in intron 4; flΔneo, allelle in which the neomycin resistance gene cassette was excised with the CRE recombinase but still possesses a *loxP* sites flanking exons 3 and 4; –, denotes the allele in which exon 3 and 4 have been removed with CRE and this also results in a frameshift mutation (Williams *et al*., 2000), which would ablate expression of the PDK1 protein beyond exon 2, which includes the kinase and pleckstrin homology domain. (**B**) The indicated ES cell lines were grown to confluence, lysed and 20 μg of protein extract was electrophoresed on a 10% SDS–polyacrylamide gel and immunoblotted with antibodies that recognize murine PDK1 (top panel) or PKBα (bottom panel). Similar results were obtained in three separate experiments. (**C**) The ES cells were lysed, and PDK1 immunoprecipitated and assayed. Data are presented as the mean of two separate experiments ± SEM with each determination carried out in triplicate.

Results

Manipulating levels of PDK1 in ES cells

We generated mouse ES cell lines called PDK1$^{fl/fl}$, in which the neomycin resistance gene flanked with the *loxP* CRE excision sites was inserted in an intron sequence between exons 2 and 3 of both alleles of the *PDK1* gene (Figure 1A). We observed that these cells were hypomorphic for PDK1 expression, as they had markedly lower levels of PDK1 protein (Figure 1B) and PDK1 kinase activity (Figure 1C) compared with the control PDK1$^{+/+}$ ES cells, while the levels of PKBα protein were identical in both cell types. Consistent with the presence of the neomycin resistance gene causing the reduction in PDK1 levels, its removal using the CRE recombinase, to generate PDK1$^{flΔneo/flΔneo}$ ES cells, resulted in restoration of PDK1 protein and kinase activity levels to those found in PDK1$^{+/+}$ ES cells. The heterozygote PDK1$^{+/fl}$ ES cells possessed a normal level of PDK1 protein and kinase activity (Figure 1B and C). The PDK1$^{+/-}$, PDK1$^{+/fl}$ and PDK1$^{+/flΔneo}$ ES cells were injected into murine blastocysts to generate mice possessing these genotypes using standard procedures.

Embryonic lethality of PDK1$^{-/-}$ mice

The PDK1$^{+/-}$ heterozygous mice were healthy and displayed no obvious phenotypes. In an attempt to generate complete PDK1 knockout mice, matings were set up between heterozygous PDK1$^{+/-}$ mice and the resulting progeny were genotyped (Table I). No PDK1$^{-/-}$ postnatal mice were ever recovered, indicating that this genotype resulted in an embryonic lethal phenotype. We next analysed the genotype of embryos from days 7.0 to 12.5 derived from PDK1$^{+/-}$ matings, which revealed the presence of PDK1$^{-/-}$ embryos at the expected Mendelian distribution at embryonic day (E) 7.5 to E9.5 (Table I). We were not able to isolate PDK1$^{-/-}$ embryos at E10 or later, indicating that the mutant embryos died and were reabsorbed after E9.5.

Therefore, to examine the pattern of PDK1 mRNA expression in E7–9 embryos, we performed whole-mount *in situ* hybridization (Figure 2). This analysis revealed that PDK1 mRNA was expressed ubiquitously in all embryonic and extra-embryonic tissues from E7 to E9.

Analysis of PDK1$^{-/-}$ phenotype

At E7.0, PDK1$^{-/-}$ embryos are already smaller than their PDK1$^{+/+}$ littermates (Figure 3A). They have defined embryonic and extra-embryonic segments, but no obvious external phenotypic difference. By E8.0 (four to six somites), PDK1$^{-/-}$ embryos are significantly smaller than their PDK1$^{+/+}$ littermates in length, possess very small headfolds, display no visible somites or posterior mesoderm, and have a small allantois. Extra-embryonic membranes are present in the PDK1$^{-/-}$ embryos. It is not clear whether these embryos have specific phenotype or are retarded in development.

However, at E8.5 (eight to 10 somites) the phenotypic differences in the PDK1$^{-/-}$ embryos become obvious. The head region is less developed, resembling a small compact mass, there are still no somites, although a presomitic mesoderm is present, and a forming neural tube is visible as is an enlarging allantois (Figure 3C).

At E9.0–9.5, the PDK1$^{+/+}$ embryos have turned and are floating inside their amniotic sacs with developed umbilical vessels. In contrast, the PDK1$^{-/-}$ embryos have not turned and lie along the top edge of their amniotic sacs with their heads indenting the membranes and interrupting the normal smooth outline (data not shown). The allantois of the E9.0 PDK1$^{-/-}$ embryos have developed further and contact the placenta and, although no vascular differentiation is seen (Figure 3D and E), blood vessels are visible in embryos and yolk sac (data not shown).

We also investigated the size of the E7.5 PDK1$^{-/-}$ and PDK1$^{+/+}$ embryonic endoderm cells using quantitative stereological procedures (see Materials and methods). This analysis revealed that PDK1$^{-/-}$ embryonic endoderm cells were markedly smaller, being only 40% of the size of wild-type cells (Figure 3F and G).

Table I. Mice matings reported in this study

Cross	Stage	Genotype	Total
$PDK1^{+/-} \times PDK1^{+/-}$	E7.5	$PDK1^{+/+}$ (25%) $PDK1^{+/-}$ (45%) $PDK1^{-/-}$ (30%)	20
$PDK1^{+/-} \times PDK1^{+/-}$	E8.5	$PDK1^{+/+}$ (27%) $PDK1^{+/-}$ (50%) $PDK1^{-/-}$ (23%)	26
$PDK1^{+/-} \times PDK1^{+/-}$	E9.5	$PDK1^{+/+}$ (23%) $PDK1^{+/-}$ (52%) $PDK1^{-/-}$ (25%)	61
$PDK1^{+/-} \times PDK1^{+/-}$	Weaning	$PDK1^{+/+}$ (34%) $PDK1^{+/-}$ (66%) $PDK1^{-/-}$ (0%)	81
$PDK1^{+/fl} \times PDK1^{+/fl}$	Weaning	$PDK1^{+/+}$ (32%) $PDK1^{+/fl}$ (47%) $PDK1^{fl/fl}$ (21%)	106
$PDK1^{fl/fl} \times PDK1^{+/-}$	Weaning	$PDK1^{+/fl}$ (63%) $PDK1^{-/fl}$ (37%)	78
$PDK1^{fl/fl} \times PDK1^{fl/fl}$	Weaning	$PDK1^{fl/fl}$ (100%)	27
$PDK1^{-/fl} \times PDK1^{-/fl}$	Weaning	$PDK1^{-/fl}$ (30%) $PDK1^{fl/fl}$ (70%) $PDK1^{-/-}$ (0%)	20

The indicated matings were set up and the progeny genotyped as described in Materials and methods. The percentage of each genotype observed is indicated in parenthesis. Total indicates the number of progeny analysed. Mice were weaned as described in Materials and methods.

To examine the phenotype of the E9–9.5 $PDK1^{-/-}$ embryos more closely, embryos were examined by scanning electron microscopy (Figure 4). This analysis revealed features of both advanced and abnormal development: the posterior growth of the $PDK1^{-/-}$ embryos seems to have halted; the somites are absent and the presomitic mesoderm appears swollen, which may be due to accumulated somitic cells (Figures 3E and 4A); the neural tube has closed, but the dorsal root ganglia are absent (Figure 4A and C); in some embryos an otic pit is clearly visible (Figure 4D), but no branchial arches are seen (Figure 4G and H); and no heart or heart tube is present (Figure 4G).

Notably, the head has developed normally to some extent in E9.5 $PDK1^{-/-}$ embryos (Figure 4D–H). The headfolds seen at earlier stages (Figure 3B) are fused, and there is a marked pre-otic sulcus and the beginnings of the open portion of the hindbrain (Figure 4E). Ventrally, the absence of the forebrain, including the eyes, is obvious (Figure 4G), a visible pit is present with the correct position and timing to be Rathke's pouch, invaginating towards the diencephalon to form the pituitary gland, which is diagnostic of a normal E9.5 embryo (Figure 4G and H). There were no detectable abnormalities in $PDK1^{+/-}$ embryos, which were indistinguishable from the $PDK1^{+/+}$ embryos.

Analysis of hypomorphic $PDK1^{fl/fl}$ and $PDK1^{-/fl}$ mutant mice

As it was not possible to generate viable $PDK1^{-/-}$ mice, we decided to breed $PDK1^{fl/fl}$ and $PDK^{-/fl}$ mice to determine whether the tissues of these mice showed reduced levels of PDK1 and whether they displayed any discernable phenotype. The $PDK1^{fl/fl}$ mice were viable and born at a marginally (~5%) lower than expected Mendelian frequency (Table I). Viable $PDK1^{-/fl}$ mice were also obtained, however, which were born at an ~25% lower frequency than predicted (Table I). Both the $PDK1^{fl/fl}$ and the $PDK1^{-/fl}$ mice were fertile (Table I). In Figure 5, we quantify the specific activities of PDK1 in eight different tissues of 4-month-old male $PDK1^{+/+}$, $PDK1^{+/-}$, $PDK1^{+/fl}$, $PDK1^{fl/fl}$, $PDK1^{-/fl}$ and $PDK1^{fl\Delta neo/fl\Delta neo}$ mice. In all tissues investigated, $PDK1^{fl/fl}$ mice had 3- to 5-fold lower PDK1 kinase activities compared with $PDK1^{+/+}$ mice, whereas $PDK1^{-/fl}$ mice had 5- to 10-fold lower PDK1 kinase activity. As expected, the PDK1 kinase activity was restored to the levels observed in wild-type animals in $PDK1^{fl\Delta neo/fl\Delta neo}$ mice in which the neomycin resistance gene had been excised. In most tissues, the $PDK1^{+/-}$ and $PDK1^{+/fl}$ mice possessed a 25–50% reduction in PDK1 activity relative to wild-type animals (Figure 5).

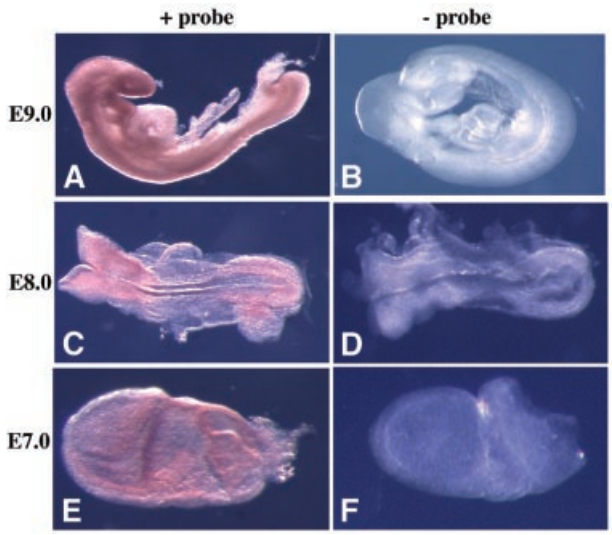

Fig. 2. PDK1 is ubiquitously expressed in early embryos. Whole-mount mRNA *in situ* hybridization for PDK1 expression was carried out on $PDK1^{+/+}$ embryos at the indicated developmental stages. The embryos were processed in the presence (+) or absence (–) of PDK1 probe. Similar results were observed in two separate experiments.

Normal activation of PKB, S6K and RSK in hypomorphic $PDK1^{-/fl}$ mice

To determine whether reduced expression of PDK1 in $PDK1^{-/fl}$ mice impaired activation of characterized PDK1 substrates, $PDK1^{+/fl}$ and $PDK1^{-/fl}$ littermates were injected with varying doses of insulin, extracts generated from skeletal muscle, liver and adipose tissue, and PKB, S6K and RSK activity was assessed (Figure 6). Activation of PKB was determined by immunoblotting cell lysates with PKB phospho-specific antibodies recognizing the T-loop PDK1 phosphorylation site (Thr308 in PKBα), as well as the hydrophobic motif (Ser473 in PKBα). There was no major difference at any of the doses of insulin used to stimulate the phosphorylation of PKB at its T-loop or hydrophobic motif in the tissues examined (Figure 6A). Even at the lowest dose of insulin that induced a detectable phosphorylation of PKB in the $PDK1^{+/fl}$ mice, a similar phosphorylation was observed in the tissues of the $PDK1^{-/fl}$ mice. S6K1 activity was examined by immuno-

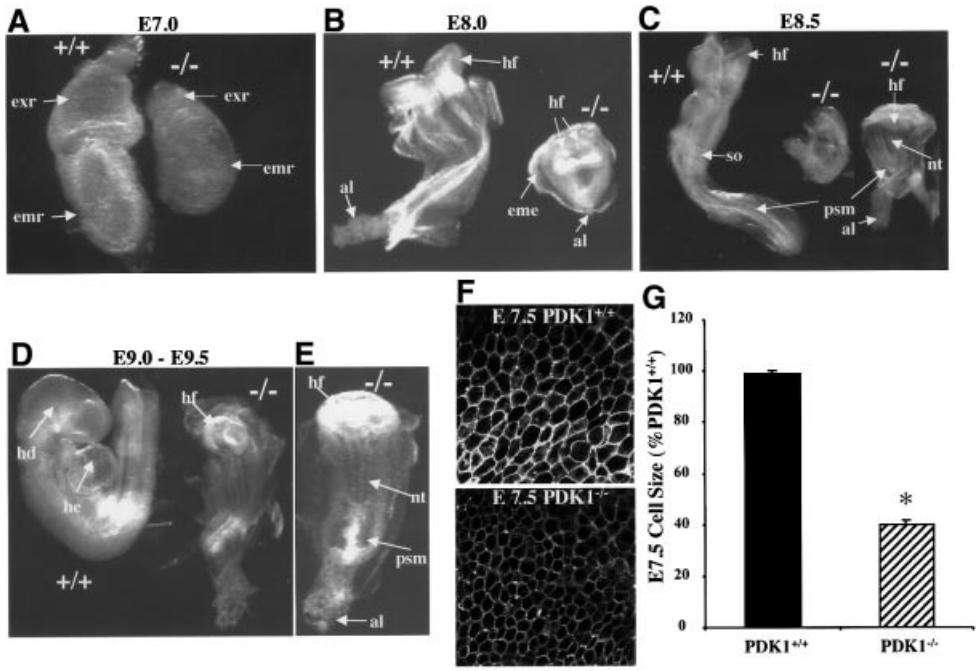

Fig. 3. Analysis of PDK1$^{-/-}$ and PDK1$^{+/+}$ embryos. (**A**–**E**) PDK1$^{-/-}$ and PDK1$^{+/+}$ embryos were dissected in PBS and imaged on a Leica M275 microscope and whole-mount photographs were taken. hd, head; hf, headfolds; he, heart; al, allantois; eme, extra-embryonic membranes; psm, presomitic mesoderm; exr, extra-embryonic region; emr, embryonic region; nt, neural tube; so, somites. (**F**) A representative image of E7.5 PDK1$^{+/+}$ and PDK1$^{-/-}$ embryonic endoderm cells stained with the lipid dye $DiIC_{16}(3)$ using a Zeiss LSM410 microscope. (**G**) The size of the E7.5 PDK1$^{+/+}$ and PDK1$^{-/-}$ embryonic endoderm cells was quantitated as described in Materials and methods. Two embryos of each genotype were analysed, with 120 cells in each embryo being measured ($P < 0.0004$).

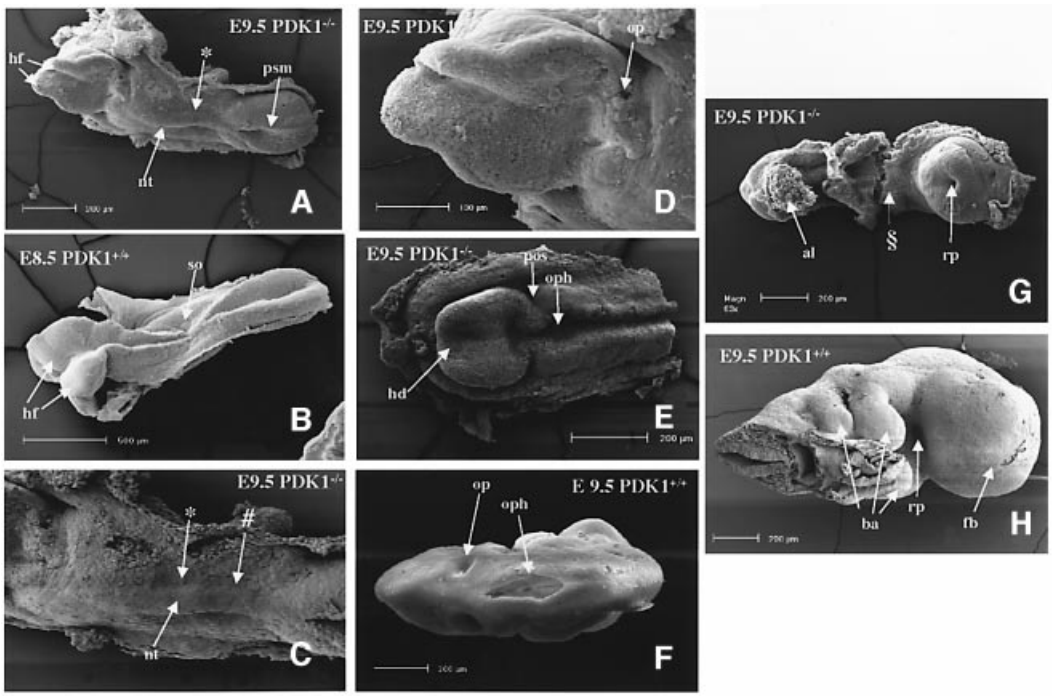

Fig. 4. Scanning electron microscope images of E8.5 PDK1$^{+/+}$ and E9.5 PDK1$^{-/-}$ embryos. Embryos were dissected into PBS and prepared for the scanning electron microscope as described in Materials and methods. (**A** and **C**–**E**) Dorsal views of E9.5 PDK1$^{-/-}$ embryos; (**F**) and (**H**) are dorsal and ventral view of a E9.5 PDK1$^{+/+}$ embryos, respectively. (**G**) A ventral view of a mutant embryo, whereas (**B**) is a dorsal view of an E8.5 PDK1$^{+/+}$ embryo. hd, head; hf, head folds; al, allantois; nt, neural tube; oph, open portion of the hindbrain; pos, pre-otic sulcus; psm, presomitic mesoderm; rp, Rathke's pouch; op, otic pit; so, somites; ba, branchial arches; fb, forebrain; *, no somites; #, no dorsal root ganglia; §, no heart.

precipitating this enzyme and measuring its ability to phosphorylate a peptide substrate (Figure 6B). The dose of insulin employed was the lowest amount that gave a significant activation of S6K1 in PDK1$^{+/+}$ mice (data not shown). These experiments revealed that S6K1 was activated similarly in PDK1$^{+/fl}$ and PDK1$^{-/fl}$ mice.

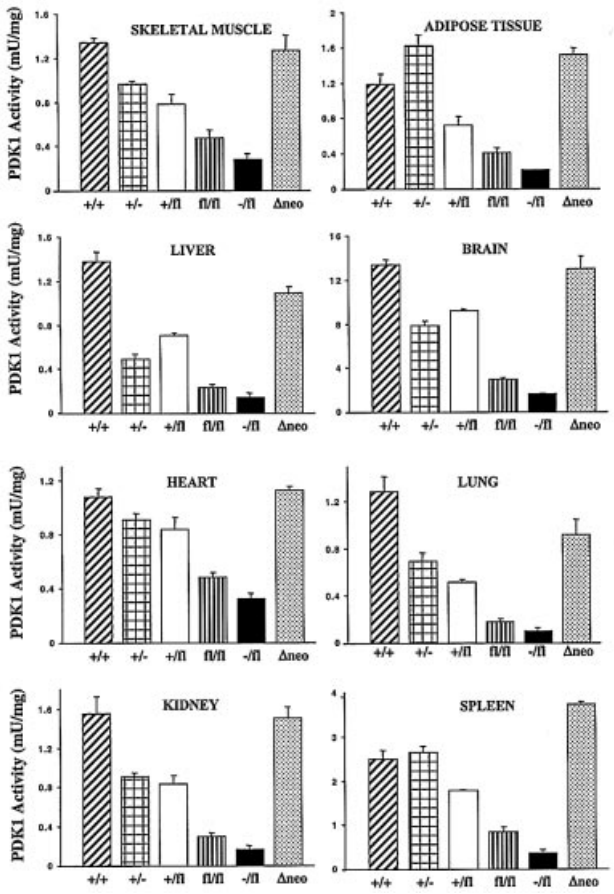

Fig. 5. Reduced PDK1 activity in PDK1$^{fl/fl}$ and PDK1$^{-/fl}$ mice. Tissue extracts from the indicated mice were prepared. PDK1 was immunoprecipitated and assayed. Data are presented as the mean ± SEM and is representative of three separate experiments with each determination carried out in triplicate. Δneo, flΔneo/flΔneo.

Insulin also stimulated ERK1 phosphorylation in skeletal muscle (Figure 6C), but not detectably in liver or adipocytes (data not shown). This enabled us to compare RSK activation in the skeletal muscle of PDK1$^{+/fl}$ and PDK1$^{-/fl}$ mice. RSK was activated similarly by insulin in both PDK1$^{+/fl}$ and PDK1$^{-/fl}$ mice (Figure 6C). We also investigated the activity of PKB, S6K and RSK isoforms in non-fasted PDK1$^{+/fl}$ and PDK1$^{-/fl}$ mice not injected with insulin. In these animals, PKB, S6K and RSK had similar basal activity in the muscle, liver and adipose tissues to the levels observed in fasted mice not injected with insulin (data not shown).

Small size of PDK1 hypomorphic mice

Both male and female hypomorphic PDK1$^{fl/fl}$ mice were ~30% smaller from birth than their PDK1$^{+/+}$ or PDK1$^{+/fl}$ littermates, and remained smaller throughout their adult life. In the case of the male mice, the difference in weight between the PDK1$^{fl/fl}$ and PDK1$^{+/+}$ mice increased to ~45% by 6 months of age, whereas the difference between the female PDK1$^{fl/fl}$ and PDK1$^{+/+}$ mice remained ~30% (Figure 7A). There was an even more marked difference in weight between the PDK1$^{-/fl}$ and PDK1$^{+/fl}$ littermates. The male and female PDK1$^{-/fl}$ mice were 45–50% and ~35%, respectively, smaller than their PDK1$^{+/+}$ littermates (Figure 7B and C). Consistent with the decrease in size of the PDK1$^{fl/fl}$ and PDK1$^{-/fl}$ mice being due to reduced levels of PDK1, both male and female PDK1$^{flΔneo/flΔneo}$ mice were similar in size to the PDK1$^{+/+}$ and PDK1$^{+/fl}$ mice (Figure 7C).

We next compared organ volumes of the kidney, pancreas, spleen and adrenal gland from PDK1$^{+/fl}$ and PDK1$^{-/fl}$ littermates using sections analysed by the quantitative Cavalieri method (Gundersen and Jensen, 1987). These four organs had an average volume that was ~50% smaller in PDK1$^{-/fl}$ mice compared with their PDK1$^{+/fl}$ littermates (Figure 7D).

Evidence that PDK1 regulates cell size

The reduced size of organs in the PDK1 hypomorphic mice could be explained if the cells are of normal size but are fewer in number and/or if the cells are smaller and just as numerous. To distinguish between these possibilities, we employed a quantitative unbiased method for determining cell volume in intact organs (as described in Materials and methods). This method uses a stereological approach called the disector principle to sample the cells in an unbiased manner before estimating their volume [other non-stereological methods of volume estimation may yield biased estimates (reviewed in Sterio, 1984; Gundersen, 1986)]. In the zona fasciculata of the adrenal gland, we found that PDK1$^{-/fl}$ cells were 45% smaller than PDK1$^{+/fl}$ cells (Figure 8B), and in Figure 8A, we show representative sections of these adrenal cells. It is important to note that the size of the nuclei in both PDK1$^{-/fl}$ and PDK1$^{+/fl}$ types was not significantly different (Figure 8A and C). Combining data on cell volume with stereological estimates of the aggregate volume of cells as described in Materials and methods, we could estimate the total number of cells in the zona fasciculata. These data showed that there was no significant difference in the number of cells in this region of the adrenal gland of the PDK1$^{+/fl}$ and PDK1$^{-/fl}$ mice (Figure 8D).

Proliferation and size of fibroblasts from PDK1-reduced expression mice

Mouse embryonic fibroblasts (MEF) were isolated from the PDK1$^{+/fl}$ and PDK1$^{-/fl}$ embryos and, consistent with other results in this study, the PDK1$^{-/fl}$ cells possessed 6-fold lower PDK1 kinase activity than PDK1$^{+/fl}$ cells (Figure 9A). We measured the size of these cells selected in disectors by the Cavalieri method (Figure 9B), and these results revealed that PDK1$^{-/fl}$ cells were 35% smaller than PDK1$^{+/fl}$ cells. We also compared the proliferation rates of the PDK1$^{+/fl}$ and PDK1$^{-/fl}$ MEF cells over a 5-day period in culture and found that there was no significant difference in the rate at which they multiplied (Figure 9C). We also analysed the viability of PDK1$^{+/fl}$ and PDK1$^{-/fl}$ MEF cells using an apoptosis TUNEL assay. Very low levels of apoptotic cells were observed in PDK1$^{+/fl}$ and PDK1$^{-/fl}$ MEF cells grown in serum, and apoptosis of these cells was induced by the addition of non-specific kinase inhibitor staurosporine. No differences in apoptosis were observed between the PDK1$^{+/fl}$ and PDK1$^{-/fl}$ MEF cells (Figure 9D). Depriving the MEF cells of serum for 24 h did not induce significant increase in basal levels of apoptosis in either cell type (data not shown).

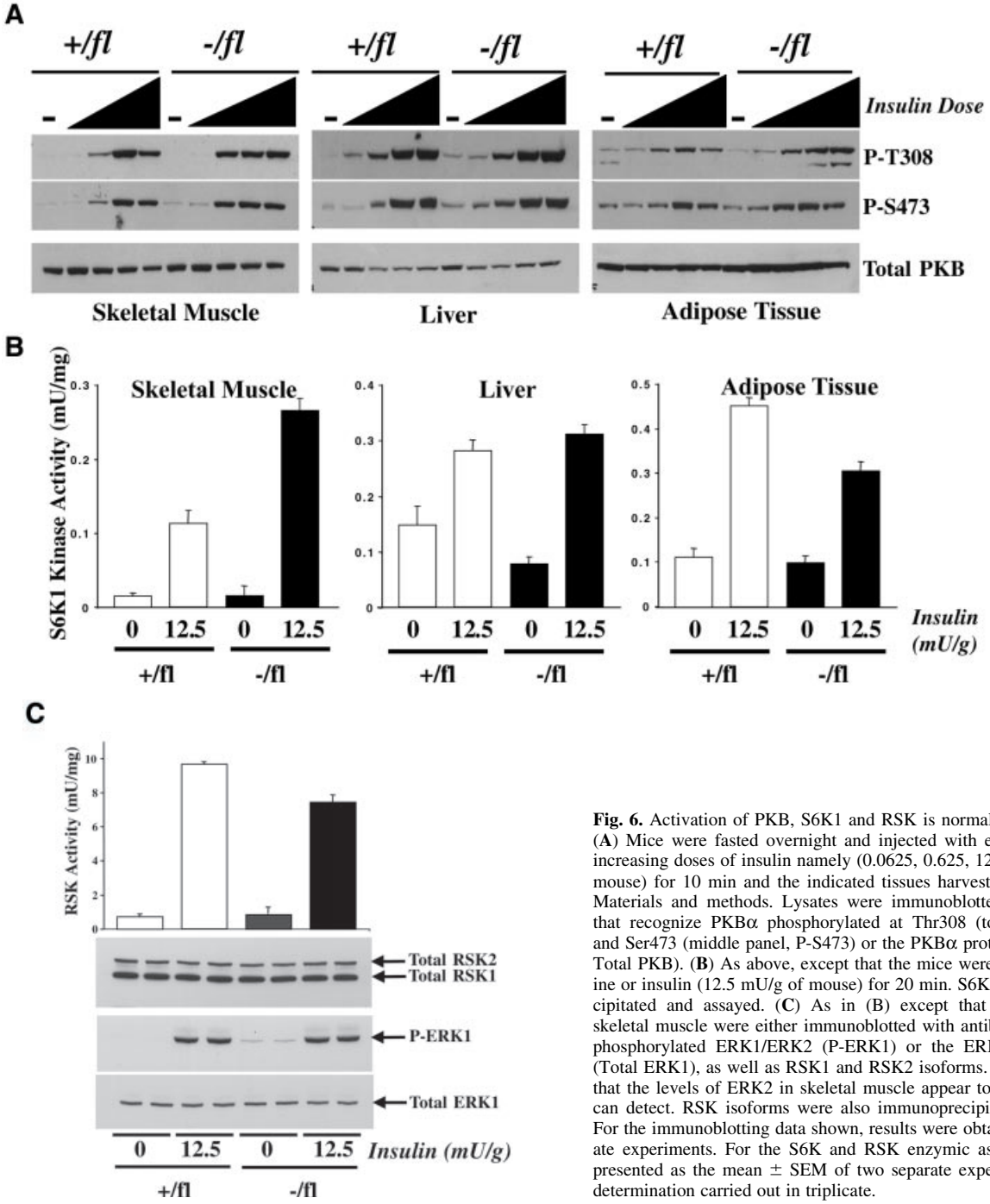

Fig. 6. Activation of PKB, S6K1 and RSK is normal in PDK1$^{-/fl}$ mice. (**A**) Mice were fasted overnight and injected with either saline (–) or increasing doses of insulin namely (0.0625, 0.625, 12.5 or 250 mU/g of mouse) for 10 min and the indicated tissues harvested as described in Materials and methods. Lysates were immunoblotted with antibodies that recognize PKBα phosphorylated at Thr308 (top panel, P-T308) and Ser473 (middle panel, P-S473) or the PKBα protein (bottom panel, Total PKB). (**B**) As above, except that the mice were injected with saline or insulin (12.5 mU/g of mouse) for 20 min. S6K1 was immunoprecipitated and assayed. (**C**) As in (B) except that cell lysates from skeletal muscle were either immunoblotted with antibodies recognizing phosphorylated ERK1/ERK2 (P-ERK1) or the ERK1/ERK2 proteins (Total ERK1), as well as RSK1 and RSK2 isoforms. It should be noted that the levels of ERK2 in skeletal muscle appear to be lower than we can detect. RSK isoforms were also immunoprecipitated and assayed. For the immunoblotting data shown, results were obtained in two separate experiments. For the S6K and RSK enzymic assays, the data are presented as the mean ± SEM of two separate experiments with each determination carried out in triplicate.

Discussion

We previously demonstrated that mouse ES cells lacking PDK1 were morphologically indistinguishable from wild-type cells and proliferated at the same rate, despite the inability of PKB, S6K and RSK to be activated in the PDK1$^{-/-}$ cells (Williams *et al*., 2000). Thus, at least for ES cells, PDK1 is not intrinsically required for survival and proliferation. However, other work has established that in yeast (Casamayor *et al*., 1999; Inagaki *et al*., 1999; Niederberger and Schweingruber, 1999), *C.elegans* (Paradis *et al*., 1999) and *Drosophila*, PDK1 homologues play a key role in regulating normal development and survival. Specifically, PDK1-deficient *Drosophila* embryos die during early larval stages (Cho,K.S. *et al*., 2001; Rintelen *et al*., 2001). Here we demonstrate, in a mammalian system, the importance of PDK1 for normal development. PDK1 is expressed ubiquitously in mouse E7–9 embryos (Figure 2). PDK1$^{-/-}$ embryos clearly complete gastrulation, are smaller and, starting at day E8.5, definite abnormalities appear including lack of somites, dorsal root ganglia, forebrain as well as posterior region development and a circulatory system. The lack of somites appears not simply to be a failure of segmentation, as there is no mesoderm lateral to the closed neural tube and there are also no branchial arches, and these could result from changes in tissue organization or cell death

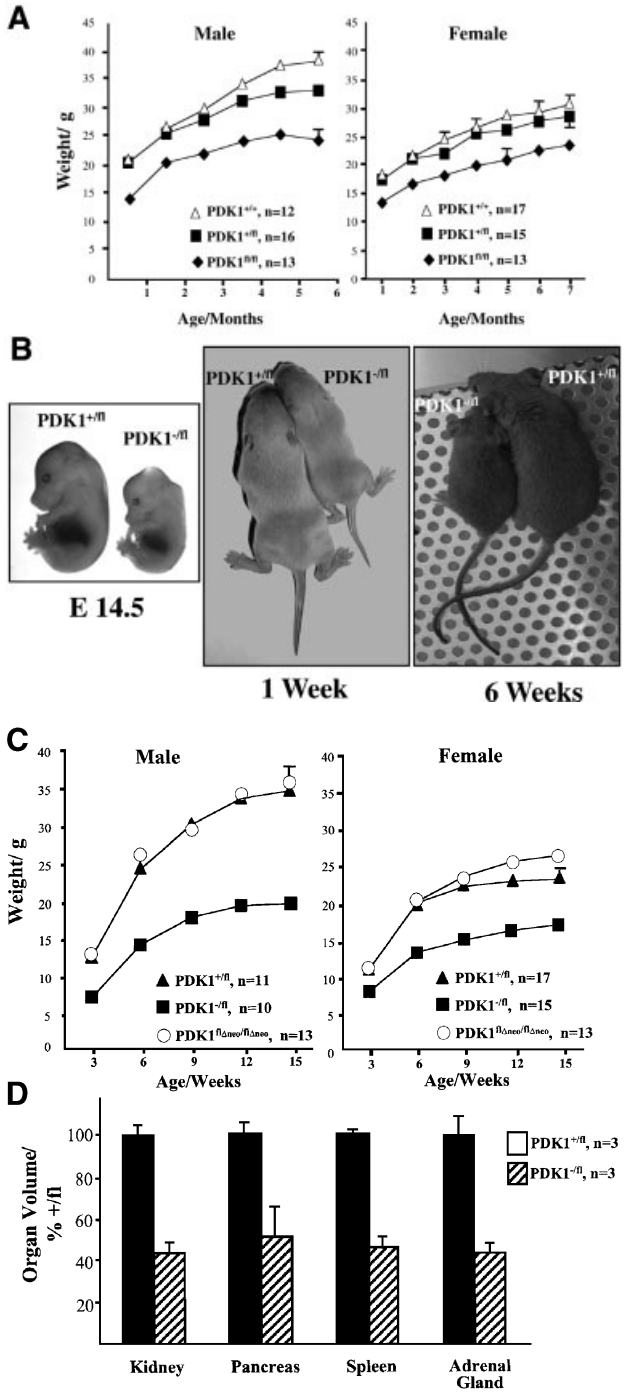

Fig. 7. Reduced size of PDK1$^{fl/fl}$ and PDK1$^{-/fl}$ mice. (**A**) The mean body weight of male and female PDK1$^{+/+}$, PDK1$^{+/fl}$ and PDK1$^{fl/fl}$ mice at the indicated age. Values represent the mean ± SEM for each data point. The numbers (*n*) of each genotype are indicated on the graph. (**B**) A representative photograph of PDK1$^{-/fl}$ and PDK1$^{+/fl}$ littermates at E14.5, 1 week and 6 weeks of age is shown. (**C**) As in (A) for the indicated mice genotypes. (**D**) The organ volume of kidney, pancreas, spleen and adrenal gland of PDK1$^{+/fl}$ and PDK1$^{-/fl}$ littermates was measured using the Cavalieri method as described in Materials and methods. The data are presented as the mean ± SEM of three different mice per genotype, and only error bars larger than the size of the symbols are shown.

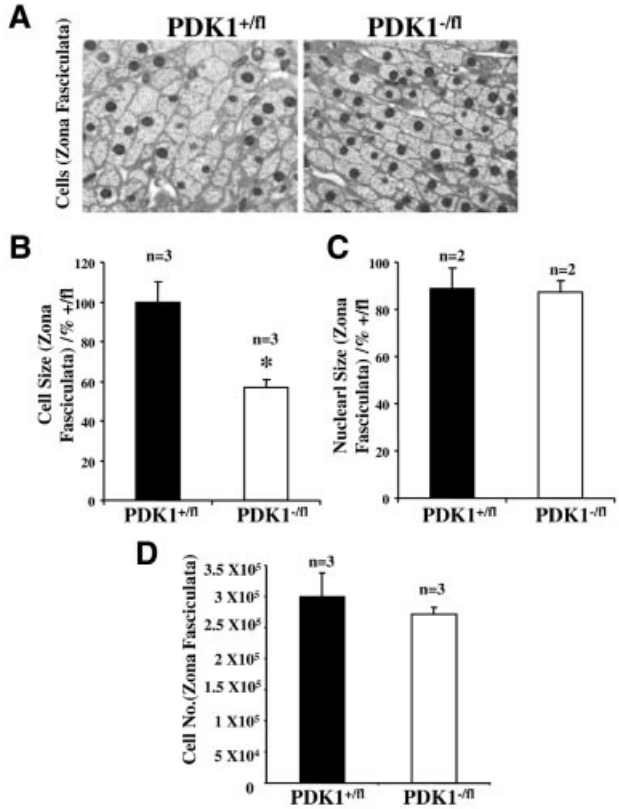

Fig. 8. PDK1$^{-/fl}$ mice possess smaller adrenal cells. (**A**) The top panel shows a micrograph (magnification ×250) of zona fasciculata cells of the adrenal gland from PDK1$^{-/fl}$ (right) and PDK1$^{+/fl}$ (left) mice. The panels are representative of the micrographs taken. (**B**) The cell size was measured using the disector principle as described in Materials and methods. The data are presented as the mean ± SEM from three separate experiments as a percentage of the PDK1$^{+/fl}$ cell size. The asterisk denotes that size of PDK1$^{-/fl}$ cells is significantly ($P < 0.005$) lower than that of PDK1$^{+/fl}$ cells. (**C**) The size of the nuclei was also measured using the disector principle. The data are presented as the mean ± SEM from two separate experiments as a percentage of the PDK1$^{+/fl}$ nuclear size. (**D**) The number of cells present in the zona fasciculata was determined by dividing the total volume of zona fasciculata cells by the volume of an individual cell. The data are presented as the mean ± SEM from three separate experiments.

(Figure 4A and C). The absence of branchial arches together with the lack of dorsal root ganglia in mutant embryos indicates a problem with neural crest specification and/or migration. No significant development posterior to the allantois is seen in PDK1$^{-/-}$ embryos, indicating that PDK1 is required for normal posterior growth and may also account for the swollen appearance of this region (Figures 3E and 4A). PDK1$^{-/-}$ embryos lack forebrain morphology and, consequently, lack eyes (Figure 4G). These observations suggest that PDK1 plays a role in forebrain specification. Interestingly, despite the absence of a forebrain, development of the mid- and hindbrain is relatively normal (Figure 4E), with fusion of the headfolds, formation of flexures and appearance of Rathke's pouch (Figure 4G). Furthermore, in PDK1$^{-/-}$ embryos, the neural tube is closed by E9.5, despite the lack of somites or dorsal root ganglia (Figure 4A and C). The cause of death appears to be due to a lack of a functional circulation. However, it should be noted that some developmental programmes in morphological regions proceed relatively normally in the absence of adjacent structures in PDK1$^{-/-}$ embryos.

Much evidence indicates that the growth and proliferation of cells is regulated by independent signalling pathways (Neufeld and Edgar, 1998; Conlon and Raff,

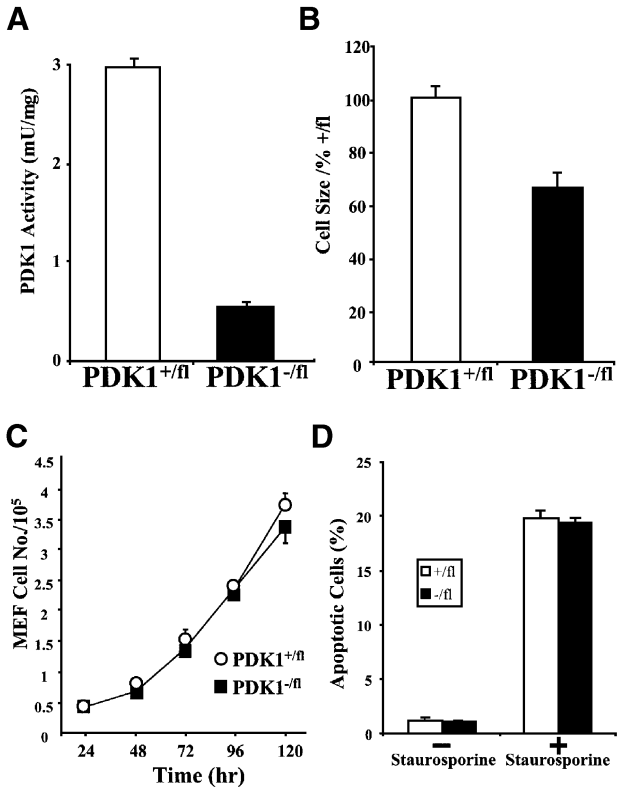

Fig. 9. PDK1$^{-/fl}$ MEF cells are smaller than PDK1$^{+/fl}$ cells but proliferate at the same rate. (**A**) PDK1 was immunoprecipitated from PDK1$^{+/fl}$ and PDK1$^{-/fl}$ cell lysates from primary MEF cells and assayed. The assays were performed in triplicate and are presented as the mean ± SEM from two separate experiments. (**B**) The size of PDK1$^{+/fl}$ and PDK1$^{-/fl}$ MEF cells was measured by the Cavalieri method as described in Materials and methods. Thirty-six PDK1$^{+/fl}$ and 32 PDK1$^{-/fl}$ cells were analysed. (**C**) Proliferation of the PDK1$^{+/fl}$ and PDK1$^{-/fl}$ MEF cells was measured as described in Materials and methods. The data are presented as the mean ± SEM from four separate experiments. (**D**) Apoptosis of the PDK1$^{+/fl}$ and PDK1$^{-/fl}$ MEF cells was measured by a TUNEL assay using the fluorescent *in situ* cell death detection method. Cells were grown to 50% confluency and then treated in the presence (+) or absence (–) of 5 μM staurosporine to induce apoptosis. The fluorescent cell death detection assay was performed in accordance with the manufacturer's instructions and 150 cells were analysed for each condition. Similar results were obtained in two experiments.

1999; Coelho and Leevers, 2000; Conlon *et al*., 2001). Some progress has been made in identifying the signalling components that participate in these processes, and elegant genetic studies in *Drosophila* have established the importance of the insulin receptor/PI 3-kinase pathway in regulating both cell size and number (reviewed in Coelho and Leevers, 2000; Kozma and Thomas, 2002). For example, the overexpression of dPI 3-kinase (Leevers *et al*., 1996; Weinkove *et al*., 1999) or inactivation of the PtdIns(3,4,5)P_3 3-phosphatase dPTEN (Goberdhan *et al*., 1999; Huang *et al*., 1999; Scanga *et al*., 2000) results in an increase in both the cell number and the cell size. Moreover, loss-of-function mutants of Chico, the fly homologue of insulin receptor substrate adaptor protein (Bohni *et al*., 1999), dPI 3-kinase or overexpression of dPTEN result in a decrease in cell size and number. More recently, a partial loss-of-function mutation in dPDK1 was shown to cause a 15% reduction in fly body weight and a 7% reduction in cell number (Rintelen *et al*., 2001). This latter observation is in contrast to our findings in the adrenal gland of PDK1 hypomorphic mice, which have a reduced zona fasciculata cell volume but the same cell number (Figure 8).

The loss-of-function mutants of dS6K1 (Montagne *et al*., 1999) or dPKB were reported to reduce *Drosophila* cell size without affecting cell number (Verdu *et al*., 1999; Scanga *et al*., 2000). PKB and S6K have also been knocked out in mice, but these studies are complicated by the presence of two isoforms of S6K (S6K1 and S6K2) and three isoforms of PKB (PKBα, PKBβ and PKBγ), encoded by distinct genes, in contrast to *Drosophila*, which have one isoform of these enzymes. Mice lacking S6K1 were viable, but adult mice were 15% smaller and possessed 10–20% reduced organ masses (Shima *et al*., 1998). It was shown subsequently that S6K1 knockout mice possessed a reduced pancreatic islet β-cell size, but that the size of other cells types investigated was apparently unaffected (Pende *et al*., 2000). Mice lacking PKBα were also reported to be 20% smaller than wild-type animals, but it was not determined whether the lack of PKBα resulted in a reduction of cell size and or cell number (Chen *et al*., 2001; Cho,H. *et al*., 2001b). In contrast, deletion of PKBβ caused insulin resistance without affecting mouse size (Cho,H. *et al*., 2001a).

The study of PDK1 in mice is facilitated by the presence of only a single isoform of this enzyme. In this study, we demonstrate that there is a strong correlation between the level of PDK1 in many diverse tissues and the overall size of the mouse and organ volumes (Figures 5 and 7). PDK1$^{-/fl}$ hypomorphic mutant mice expressing ~10–20% of the normal level of PDK1 are 40–50% smaller and possess proportionately reduced organ volumes (Figure 7). Despite this, the PDK1$^{-/fl}$ mice are healthy and are even fertile (Table I).

By using quantitative methodologies, we have demonstrated that in the adrenal gland of PDK1$^{-/fl}$ animals, there are the same number of zona fasciculata cells, but they are 45% smaller. Interestingly, the size of the nucleus is identical in both PDK1$^{-/fl}$ and PDK1$^{+/fl}$ zona fasciculata cells, suggesting that the reduction of PDK1 is caused by a specific reduction in cytoplasmic volume. Thus, pathways regulating nuclear size are independent of those controlling cytoplasmic volume. Consistent with cell size being a genetic determinant of the cell itself, we show that primary MEF cells cultured from PDK1$^{-/fl}$ mice are also 35% smaller than cells derived from PDK1$^{+/fl}$ animals (Figure 9B). In agreement with separate pathways regulating cell size and proliferation (Conlon and Raff, 1999; Coelho and Leevers, 2000), we find that PDK1$^{-/fl}$ and PDK1$^{+/fl}$ MEF cells proliferate at the same rate, despite being different sizes (Figure 9C). The key role of PDK1 in regulating cell size is emphasized by the finding that embryonic endoderm cells completely lacking PDK1 are 60% smaller than wild-type cells (Figure 3F and G).

A key question to address is: what is the mechanism by which PDK1 is regulating cell size in mammalian cells? Our data suggest that although the levels and activity of PDK1 are markedly reduced in the PDK1$^{-/fl}$ mice, injection of these animals with low doses of insulin can still induce normal activation of PKB and S6K in liver, adipose and skeletal muscle (Figure 6). As discussed in the

Introduction, PDK1 also plays a key role in regulating the activity of the RSK AGC kinase, but RSK isoforms are activated to a similar extent in skeletal muscle of $PDK1^{-/fl}$ and $PDKl^{fl/fl}$ mice following an injection of insulin. Furthermore, we have found, in $PDK1^{fl/fl}$ ES cells (Figure 1) and $PDK1^{-/fl}$ MEF cells (Figure 9) that possess markedly reduced levels of PDK1, that IGF1 induced activation of PKB and S6K is normal, as is TPA-induced activation of RSK (M.A.Lawlor, unpublished data). Therefore, in the PDK1 hypomorphic mice, as well as in ES and MEF cells, there is still sufficient PDK1 present to trigger the normal phosphorylation of three of its known insulin-stimulated substrates. These observations may indicate that PDK1 can regulate cell size independently of S6K, PKB or RSK. However, it cannot be ruled out that the levels of PDK1 in the hypomorphic mice are not sufficient to fully activate PKB, S6K or RSK in response to unknown endogenous stimuli regulating cell size during tissue development. It has also been suggested that PDK1 can interact via its non-catalytic N-terminus with the PI 3-kinase-regulated Ral GTP exchange factor leading to its activation (Tian *et al*., 2002). To our knowledge, the Ral GTPase has not been implicated in regulating cell size, but it may be important to investigate whether activation of Ral GTPases is defective in PDK1 hypomorphic mice in future studies. Recently, mice lacking the p190-B Rho GTPase have been found to be 30% smaller, and it was suggested that this reduction in size was mediated through phosphorylation of the transcription factor CREB at Ser133 (Sordella *et al*., 2002). We analysed CREB phosphorylation in various tissues of the $PDK1^{+/fl}$ and $PDK1^{-/fl}$ mice and did not observe any significant differences (data not shown), indicating that PDK1 is not regulating cell size by this mechanism.

In conclusion, we provide firm genetic evidence that PDK1 is required for mammalian embryonic development, as a complete lack of PDK1 in embryos results in multiple defects culminating in embryonic lethality. Interestingly, levels of PDK1 up to 10-fold lower than those found in wild-type mice are sufficient to enable embryos to develop normally, producing viable and fertile animals. However, a reduction of PDK1 levels in mice that is insufficient to affect activation of PKB, S6K or RSK in response to insulin injection has a large effect on their overall body and organ size, and this effect appears to operate principally by a reduction in cell size rather than number. A key challenge for future research is to define the mechanism by which PDK1 can regulate cell size in mammals.

Materials and methods

Materials

Taq DNA polymerase was purchased from Promega. Protease inhibitor cocktail tablets, DNA molecular weight markers, T7 RNA polymerase, the Fluorescent In Situ Cell Death Detection Kit and digoxygenin RNA labelling mix were supplied by Roche. Bradford reagent was supplied by Pierce and staurosporine was from Calbiochem. Human insulin was purchased from Novo Nordisk and electron microscopy grade glutaraldehyde was purchased from Sigma. The lipid dye 1,1′-dihexadecyl-3,3,3′,3′-tetramethylindocarbocyanine perchlorate [$DiIC_{16}(3)$] was purchased from Molecular Probes.

Antibodies

The phospho-specific antibodies that recognize PKB phosphorylated at Ser473 and Thr308 and total and activated ERK1/ERK2 were from Cell Signalling. The anti-digoxigenin–AP, Fab fragment antibody was supplied by Roche Molecular Biochemicals. The PDK1 antibody was raised against the sequence RKIQEVWRQQYQSNPDAAVQ (residues 540–559 of mouse PDK1; Williams *et al*., 2000); antibodies that recognize S6K1 were raised against residues 1–421 (containing T412E and a His tag) of the human protein. The PKB total antibody was raised against the sequence RPHFPQFSYSASGTA (residues 466–480) of rat PKBα and antibodies against that recognize isoforms of RSK were raised against the peptide RNQSPVLEPVGRSTLAQRRGIKK (residues 712–734) of human RSK2.

Generation and genotype analysis of chimeric and mutant mice

ES cell lines for $PDK1^{+/fl}$, $PDK1^{+/-}$ and $PDK1^{fl\Delta neo/fl\Delta neo}$ were produced as described previously (Williams *et al*., 2000). Chimeric mice were generated using standard protocols. Briefly, heterozygous ES cell clones for $PDK1^{+/fl}$, $PDK1^{+/-}$ and $PDK1^{fl\Delta neo/fl\Delta neo}$ were injected into C57Black6 × Balb/c blastocysts, which were then re-implanted into recipient female mice. Chimeric mice, which showed a high degree of ES cell contribution were identified by coat colour and were subsequently crossed to Balb/c mice and heterozygous mice, were identified by a grey coat. Genotyping was performed by PCR using genomic DNA isolated from tails or embryonic membranes. The presence of a wild-type allele was detected using two primers located in fourth intron [sense primer (p99), 5′-ATCCCAAGTTACTGAGTTGTGTTGGAAG-3′; anti-sense primer (p100r), 5′-TGTGGACAAACAGCAATGAACATACACGC-3′; see Figure 1A]. The presence of the PDK1 (fl) allele was detected using a primer specific for the neomycin resistance gene and one present in the second intron of the *PDK1* gene [sense primer (p80), 5′-CTATGC-TGTGTTACTTCTTGGAGCACAG-3′; anti-sense primer (p81r), 5′-TGCCGAATATCATGGTGGAAAATGGCCG-3′; see Figure 1A]. The PDK1 (–) allele was detected using the primers p80 and p100r (see Figure 1A). Thirty cycles (denaturation 1 min, 94°C; annealing 2 min, 63°C; elongation 3 min, 72°C) were performed and the amplified products were separated by 2% agarose gel electrophoresis.

Whole-mount in situ hybridization

Noon of the day of the vaginal plug was considered as 0.5 days post-coital in the timing of the embryos. When removed from the decidua, embryos were staged according to morphological criteria (Kaufman, 1992) and genotyped as described above. Embryos were fixed overnight in 4% paraformaldehyde in phosphate-buffered saline (PBS), and whole-mount *in situ* hybridization was carried out using digoxigenin-UTP-labelled single-stranded RNA probes as described previously (Wilkinson, 1992). The PDK1 RNA probe was generated by subcloning a 1.45 kb *Bam*H1–*Bam*H1 fragment corresponding to nucleotides 245–1687 of the mouse PDK1 cDNA (DDBJ/EMBL/GenBank accession No. NM_011062) into the pBSks plasmid. The 0.7 kb anti-sense RNA probe was generated using T7 RNA polymerase after linearizing the plasmid with *Bgl*I.

Scanning electron microscopy

Embryos were fixed in 1.25% glutaraldehyde, 1% paraformaldehyde in 0.08 M cacodylate buffer pH 7.2 containing 0.02% $CaCl_2$ for 1 h at room temperature and overnight at 4°C. They were subsequently washed in cacodylate buffer, post-fixed in 1% OsO_4 in water, washed and dehydrated by alcohol using a standard protocol. The embryos were then transferred into 100% acetone and critical point dried. Finally, they were coated with Au/Pd and imaged in an FEI XL30 ESEM in high vacuum mode.

Determination of organ volume, cell size and cell number

Organ volume was determined using the Cavalieri method (Gundersen and Jensen, 1987). In brief, the spleen, kidney and pancreas were harvested and fixed by immersion in 10% formalin, neutral buffered saline solution, before embedding in paraffin wax. The adrenal gland was fixed in PBS containing paraformaldehyde (4%) and glutaraldehyde (1%) at 4°C for at least 1 day and then embedded in epoxy resin. Sections were taken at systematically spaced locations from a random starting position (see below). The sections thickness was 7 μm (spleen kidney and pancreas) and 1 μm (adrenal gland). The sections were stained with either haematoxylin and eosin (spleen, kidney, pancreas) or Richardson's stain (adrenal gland) and pictures were taken either on an Zeiss Axioscope microscope (40× magnification) using a digital camera or microscope

slides scanned directly at 2000 d.p.i. on a flat-bed scanner in transmission mode. A square lattice grid was then overlayed on the picture using the program Photoshop version 4.0 or 5.5 and the number of points (grid square corners) (*P*) hitting the organ was counted (*P* ranged from 250 to 600 for $PDK1^{-/fl}$ and $PDK1^{+/fl}$ mice, respectively). The organ volume was then estimated using the following equation:

$$\sum P \times d^2 \times k$$

in which *d*, the distance between each point of the square lattice grid, was 500 μm for spleen, kidney and pancreas and 134 μm for adrenal gland. For spleen, kidney and pancreas the spacing, *k*, between each section was 350–450 μm, and for adrenal this value was 150 μm.

The cell size of the E7.5 $PDK1^{+/+}$ and $PDK1^{-/-}$ embryos was measured using the Cavalieri method. Embryos were dissected into PBS and fixed in 1.0% glutaraldehyde, 1% paraformaldehyde in 0.08 M cacodylate buffer pH 7.2 containing 0.02% $CaCl_2$ for 1 h at room temperature followed by an overnight incubation at 4°C. The embryos were washed three times in PBS, and stained for 1 h at room temperature with the lipid dye 1,1′-dihexadecyl-3,3,3′,3′-tetramethylindocarbocyanine perchlorate [$DiIC_{16}(3)$] at 50 μg/ml in PBS. Four to five Z-series (20 sections per series) were taken at random locations approximately orthogonal to the most peripheral single cell layer of the embryonic endoderm using a Zeiss LSM410 microscope. Cell profiles were selected by applying the forbidden line two-dimensional counting rule to sampling quadrants placed over the cell sheet in the Z-series. The volume was determined as described above, with *P* ranging from 30 to 40; *d* was 2.25 μm and *k* was 1 μm. At least 10 sections were analysed for each cell.

MEF cell size was also measured using the Cavalieri method. Cells were grown to 50% confluence, trypsinized, pelleted and overlayed with fixative (PBS with 1% glutaraldehyde). After embedding in epoxy resin, semi-thin (0.2 μm) sections were cut, stained with Richardson's stain and pictures take at 100× magnification. The volume was determined on disector selected cells as described above, with *P* ranging from 45 to 110; *d* was 2.85 μm and *k* was 2 μm. At least six to seven sections were analysed for each cell.

The volume of cells and nuclei in zona fasciculata layer of the adrenal gland was estimated using the disector principle (Sterio, 1984; Gundersen, 1986). The adrenal gland was isolated, fixed in PBS containing paraformaldehyde (4%) and glutaraldehyde (1%) and embedded in resin. Pairs of sequential 1.0-μm sections were taken at five or six systematically spaced locations throughout the organ. These sections were photographed at a 250× magnification and sampling quadrates applied to sections across the thickness of the fasciculata layer in Photoshop 4.0 or 5.5 to each of the sections in turn. Nuclear profiles belonging to fasciculata cells (endothelial cell nuclei were ignored) were selected according to the forbidden-line two-dimensional unbiased counting rule and counted as Q^- if they disappeared in the adjacent look-up section. Using the disectors in both directions increases efficiency. For each $PDK1^{-/fl}$ adrenal gland, Q^- ranged between 90 and 115, and for $PDK1^{+/fl}$ adrenal glands, 40–55 Q^- were counted. The total volume of cell space projected into the disector from each counting frame was estimated using point counting with a square lattice grid (spacing 10 μm). The cell volume was calculated using the formula:

$$(\sum P/\sum Q^-) \times d^2 \times t$$

in which *P* is the number of points hitting the fasciculata cell cytoplasm and nucleus, *d* is the distance between two points on the square lattice grid (10 μm), and *t* is the section thickness. The volume of the nucleus was also measured using the disector principle with one difference: *P* is the number of points hitting the zona fasciculata cell nucleus only. The number of cells in the zona fasciculata was calculated by dividing the total volume of the zona fasciculata cells (determined as described above using Cavalieri's estimator) by the volume of an individual cell for that organ.

Tissue cell culture

Primary MEF cells were isolated from E13.5 embryos and cultured by standard procedures. The cells were not used beyond passage five. Cell proliferation was measured by plating the MEF cells from each genotype at a density of 1.25×10^5 onto a 3.5-cm diameter, 6-well plate. Cells were trypsinized at 24-h intervals and the number of cells counted using a hematocytometer. ES cells were cultured and lysed as described previously (Williams *et al*., 2000).

Preparation of tissue extracts, immunoblotting and protein kinase assays

Following an overnight fast, a bolus of insulin or saline solution was injected via the inferior vena cava of terminally anaesthetized mice. Adipose, gastrocnemius and quadriceps (pooled) skeletal muscle and liver tissue were harvested after either 10 min (PKB) or 20 min (S6K1 and p90 RSK) of stimulation, and immediately snap frozen in liquid nitrogen. The tissues were stored at –80°C and homogenized to a powder in liquid nitrogen. A 5-fold mass excess of ice-cold 50 mM Tris–HCl pH 7.5, 1 mM EDTA, 1 mM EGTA, 1% (w/v) Triton X-100, 0.1% (v/v) β-mercaptoethanol, 1 mM sodium orthovanadate, 50 mM sodium fluoride, 5 mM sodium pyrophosphate, 1 μM microcystin-LR and one tablet of 'complete' proteinase inhibitor per 50 ml of buffer, was added to the powdered tissue, incubated on ice for 30 min and then centrifuged at 4°C for 5 min at 13 000 *g* to remove insoluble material. The supernatant was snap frozen in aliquots in liquid nitrogen and stored at –80°C. The activation state of PKB, S6K and RSK isoforms were assessed by immunoblotting extracts (20 μg) with the indicated phosphospecific antibodies and following their immunoprecipitation from cell extracts as described previously (Williams *et al*., 2000).

Acknowledgements

We would like to thank Professor Cheryll Tickle for numerous helpful discussions and for critical reading of the manuscript. We thank the Operations Team of the Division of Signal Transduction Therapy (DSTT) for preparation of antibodies, Agnieszka Kieloch for assistance with tissue culture, Calum Thomson for technical help in the cell size studies, and Birgit Lane and Angus Lamond for use of microscopes. J.M.L. is supported by a Research Leave Fellowship from the Wellcome Trust (059767/Z/99/Z) and D.R.A. acknowledges the support of the Association for International Cancer Research, Diabetes UK, the UK Medical Research Council, and the pharmaceutical companies supporting the DSTT unit in Dundee (AstraZeneca, Boehringer Ingelheim, GlaxoSmithKline, Novo-Nordisk and Pfizer).

References

Alessi,D.R. (2001) Discovery of PDK1, one of the missing links in insulin signal transduction. *Biochem. Soc. Trans*, **29**, 1–14.

Avruch,J., Belham,C., Weng,Q., Hara,K. and Yonezawa,K. (2001) The p70 S6 kinase integrates nutrient and growth signals to control translational capacity. *Prog. Mol. Subcell. Biol.*, **26**, 115–154.

Biondi,R.M., Kieloch,A., Currie,R.A., Deak,M. and Alessi,D.R. (2001) The PIF-binding pocket in PDK1 is essential for activation of S6K and SGK, but not PKB. *EMBO J.*, **20**, 4380–4390.

Bohni,R., Riesgo-Escovar,J., Oldham,S., Brogiolo,W., Stocker,H., Andruss,B.F., Beckingham,K. and Hafen,E. (1999) Autonomous control of cell and organ size by CHICO, a *Drosophila* homolog of vertebrate IRS1-4. *Cell*, **97**, 865–875.

Brazil,D.P. and Hemmings,B.A. (2001) Ten years of protein kinase B signalling: a hard Akt to follow. *Trends Biochem. Sci.*, **26**, 657–664.

Casamayor,A., Torrance,P.D., Kobayashi,T., Thorner,J. and Alessi,D.R. (1999) Functional counterparts of mammalian protein kinases PDK1 and SGK in budding yeast. *Curr. Biol.*, **9**, 186–197.

Chen,W.S. *et al*. (2001) Growth retardation and increased apoptosis in mice with homozygous disruption of the Akt1 gene. *Genes Dev.*, **15**, 2203–2208.

Cho,H. *et al*. (2001a) Insulin resistance and a diabetes mellitus-like syndrome in mice lacking the protein kinase Akt2 (PKB β). *Science*, **292**, 1728–1731.

Cho,H., Thorvaldsen,J.L., Chu,Q., Feng,F. and Birnbaum,M.J. (2001b) Akt1/PKBα is required for normal growth but dispensable for maintenance of glucose homeostasis in mice. *J. Biol. Chem.*, **276**, 38349–38352.

Cho,K.S., Lee,J.H., Kim,S., Kim,D., Koh,H., Lee,J., Kim,C., Kim,J. and Chung,J. (2001) *Drosophila* phosphoinositide-dependent kinase-1 regulates apoptosis and growth via the phosphoinositide 3-kinase-dependent signaling pathway. *Proc. Natl Acad. Sci. USA*, **98**, 6144–6149.

Coelho,C.M. and Leevers,S.J. (2000) Do growth and cell division rates determine cell size in multicellular organisms? *J. Cell Sci.*, **113**, 2927–2934.

Conlon,I. and Raff,M. (1999) Size control in animal development. *Cell*, **96**, 235–244.

Conlon,I.J., Dunn,G.A., Mudge,A.W. and Raff,M.C. (2001) Extracellular control of cell size. *Nat. Cell Biol.*, **3**, 918–921.

Frodin,M. and Gammeltoft,S. (1999) Role and regulation of 90 kDa ribosomal S6 kinase (RSK) in signal transduction. *Mol. Cell. Endocrinol.*, **151**, 65–77.

Frodin,M., Jensen,C.J., Merienne,K. and Gammeltoft,S. (2000) A phosphoserine-regulated docking site in the protein kinase RSK2 that recruits and activates PDK1. *EMBO J.*, **19**, 2924–2934.

Goberdhan,D.C., Paricio,N., Goodman,E.C., Mlodzik,M. and Wilson,C. (1999) *Drosophila* tumor suppressor PTEN controls cell size and number by antagonizing the Chico/PI3-kinase signaling pathway. *Genes Dev.*, **13**, 3244–3258.

Gundersen,H.J. (1986) Stereology of arbitrary particles. A review of unbiased number and size estimators and the presentation of some new ones, in memory of William R. Thompson. *J. Microsc.*, **143**, 3–45.

Gundersen,H.J. and Jensen,E.B. (1987) The efficiency of systematic sampling in stereology and its prediction. *J. Microsc.*, **147**, 229–263.

Huang,H., Potter,C.J., Tao,W., Li,D.M., Brogiolo,W., Hafen,E., Sun,H. and Xu,T. (1999) PTEN affects cell size, cell proliferation and apoptosis during *Drosophila* eye development. *Development*, **126**, 5365–5372.

Inagaki,M., Schmelzle,T., Yamaguchi,K., Irie,K., Hall,M.N. and Matsumoto,K. (1999) PDK1 homologs activate the Pkc1-mitogen-activated protein kinase pathway in yeast. *Mol. Cell. Biol.*, **19**, 8344–8352.

Kaufman,M.H. (1992) *The Atlas of Mouse Development*. Academic Press, London, UK.

Kozma,S.C. and Thomas,G. (2002) Regulation of cell size in growth, development and human disease: PI3K, PKB and S6K. *BioEssays*, **24**, 65–71.

Lawlor,M.A. and Alessi,D.R. (2001) PKB/Akt: a key mediator of cell proliferation, survival and insulin responses? *J. Cell Sci.*, **114**, 2903–2910.

Leevers,S.J., Weinkove,D., MacDougall,L.K., Hafen,E. and Waterfield,M.D. (1996) The *Drosophila* phosphoinositide 3-kinase Dp110 promotes cell growth. *EMBO J.*, **15**, 6584–6594.

Montagne,J., Stewart,M.J., Stocker,H., Hafen,E., Kozma,S.C. and Thomas,G. (1999) *Drosophila* S6 kinase: a regulator of cell size. *Science*, **285**, 2126–2129.

Nebreda,A.R. and Gavin,A.C. (1999) Perspectives: signal transduction. Cell survival demands some Rsk. *Science*, **286**, 1309–1310.

Neufeld,T.P. and Edgar,B.A. (1998) Connections between growth and the cell cycle. *Curr. Opin. Cell Biol.*, **10**, 784–790.

Niederberger,C. and Schweingruber,M.E. (1999) A *Schizosaccharomyces pombe* gene, *ksg*1, that shows structural homology to the human phosphoinositide-dependent protein kinase PDK1, is essential for growth, mating and sporulation. *Mol. Gen. Genet.*, **261**, 177–183.

Paradis,S., Ailion,M., Toker,A., Thomas,J.H. and Ruvkun,G. (1999) A PDK1 homolog is necessary and sufficient to transduce AGE-1 PI3 kinase signals that regulate diapause in *Caenorhabditis elegans*. *Genes Dev.*, **13**, 1438–1452.

Pende,M., Kozma,S.C., Jaquet,M., Oorschot,V., Burcelin,R., Le Marchand-Brustel,Y., Klumperman,J., Thorens,B. and Thomas,G. (2000) Hypoinsulinaemia, glucose intolerance and diminished β-cell size in S6K1-deficient mice. *Nature*, **408**, 994–997.

Rintelen,F., Stocker,H., Thomas,G. and Hafen,E. (2001) PDK1 regulates growth through Akt and S6K in *Drosophila*. *Proc. Natl Acad. Sci. USA*, **98**, 15020–15025.

Scanga,S.E. *et al*. (2000) The conserved PI3′K/PTEN/Akt signaling pathway regulates both cell size and survival in *Drosophila*. *Oncogene*, **19**, 3971–3977.

Scheid,M.P. and Woodgett,J.R. (2001) Pkb/akt: functional insights from genetic models. *Nat. Rev. Mol. Cell Biol.*, **2**, 760–768.

Shima,H., Pende,M., Chen,Y., Fumagalli,S., Thomas,G. and Kozma,S.C. (1998) Disruption of the $p70^{s6k}/p85^{s6k}$ gene reveals a small mouse phenotype and a new functional S6 kinase. *EMBO J.*, **17**, 6649–6659.

Sordella,R. *et al*. (2002) Modulation of CREB activity by the Rho GTPase regulates cell and organism size during mouse embryonic development. *Dev. Cell*, **2**, 553–565.

Sterio,D.C. (1984) The unbiased estimation of number and sizes of arbitrary particles using the disector. *J. Microsc.*, **134**, 127–136.

Tian,X., Rusanescu,G., Hou,W., Schaffhausen,B. and Feig,L.A. (2002) PDK1 mediates growth factor-induced Ral-GEF activation by a kinase-independent mechanism. *EMBO J.*, **21**, 1327–1338.

Toker,A. and Newton,A.C. (2000) Cellular signaling: pivoting around PDK1. *Cell*, **103**, 185–188.

Verdu,J., Buratovich,M.A., Wilder,E.L. and Birnbaum,M.J. (1999) Cell-autonomous regulation of cell and organ growth in *Drosophila* by Akt/PKB. *Nat. Cell Biol.*, **1**, 500–506.

Volarevic,S. and Thomas,G. (2001) Role of S6 phosphorylation and S6 kinase in cell growth. *Prog. Nucleic Acid Res. Mol. Biol.*, **65**, 101–127.

Weinkove,D., Twardzik,T., Waterfield,M.D. and Leevers,S.J. (1999) The *Drosophila* class IA phosphoinositide 3-kinase and its adaptor are autonomously required for imaginal discs to achieve their normal cell size, cell number and final organ size. *Curr. Biol.*, **9**, 1019–1029.

Wilkinson,D.G. (1992) *In Situ Hybridisation: A Practical Approach*. IRL Press, Oxford, UK.

Williams,M.R., Arthur,J.S., Balendran,A., van der Kaay,J., Poli,V., Cohen,P. and Alessi,D.R. (2000) The role of 3-phosphoinositide-dependent protein kinase 1 in activating AGC kinases defined in embryonic stem cells. *Curr. Biol.*, **10**, 439–448.

Received April 2, 2002; revised and accepted May 30, 2002